



Cite this: DOI: 10.1039/c8dt03941k

# Living/controlled ring-opening (co)polymerization of lactones by Al-based catalysts with different sidearms†

Wuchao Zhao, Qianyi Wang, Yunpeng Cui, Jianghua He and Yuetao Zhang \*

It remains a challenging task to synthesize well-defined multi-block copolymers through the controlled/living ring-opening polymerization (ROP) of lactones without transesterification, the most common side reaction occurring during copolymerization. A series of Al-based complexes with different sidearms were prepared for living ROP of lactones such as  $\epsilon$ -caprolactone ( $\epsilon$ -CL) and  $\delta$ -valerolactone ( $\delta$ -VL) in the presence of BnOH at room temperature (RT), affording medium to high molecular weight (MW) linear polyesters with  $M_w$  up to 303 kg mol<sup>-1</sup> and narrow molecular weight distributions (MWD,  $\bar{D}$  as low as 1.12). The coordination–insertion polymerization mechanism was proposed based on the combination of the detailed experimental data and polymerization kinetics. It should be noted that the sidearm plays a significant important role in the reactivity of these Al-based catalyst systems. More specifically, the **Al2** system with a butyl substituent on the sidearm exhibited the highest polymerization activity and the **Al5** system with the bulkiest sidearm showed the lowest one among the investigated catalysts. Moreover, the **Al4** system with a pyridine group on the sidearm could effectively inhibit transesterification and maintain a well-defined block copolymer structure even after heating at 50 °C for 10 h, which could also be confirmed by chain-end analyses of the produced polymers with the MALDI-TOF MS measurement.

Received 30th September 2018,  
Accepted 15th November 2018

DOI: 10.1039/c8dt03941k

rsc.li/dalton

## Introduction

Aliphatic (co)polyesters derived from sustainable monomers<sup>1–5</sup> have attracted much intense attention due to various applications in biomedicine, drug delivery, temporary implants for tissue engineering, and food technologies (*e.g.*, for packaging) resulting from their biocompatible, biodegradable and permeability properties.<sup>6</sup> As a powerful polymerization technique that combines the ability to produce condensation-type polymers with fast chain-growth polymerization kinetics, ring-opening polymerization (ROP) of lactones has been widely utilized to produce aliphatic polyesters.<sup>2,7–14</sup> Different types of catalysts have been developed for the synthesis of such (co) polyesters, such as organic complexes<sup>9,10,15,16</sup> and metal-based systems.<sup>3,14,17–20</sup> However, many of them produced random or gradient-block copolymers with medium MW instead of well-defined block copolymers.<sup>15,21–27</sup> Therefore, it remains a challenging task to synthesize advanced polymers such as multi-

block copolymers or sequence-controlled block copolymers. Moreover, the most common side reaction, transesterification, often occurred along with the copolymerization, leading to random copolyesters.<sup>28</sup> In general, well-defined block copolymers could be synthesized by strictly controlled experimental conditions, such as reaction time and temperature. It might also be realized by choosing a suitable combination of Lewis base (LB) and Lewis acid (LA) for polymerization. Recently, our group utilized Lewis pairs (LPs) composed of strong LA Al(C<sub>6</sub>F<sub>5</sub>)<sub>3</sub> with a strong LB N-heterocyclic olefin to synergistically promote living ring-opening (co)polymerization of lactones and successfully produced a well-defined block copolymer of  $\epsilon$ -CL and  $\delta$ -VL without transesterification.<sup>29</sup> However, more effective catalyst systems are still needed to accomplish this goal without occurrence of the transesterification side reaction.

Organometallic catalysts are of particular interest due to their easy-tunable ligand structure and excellent catalytic performance. Both stability and catalytic performance of metal-based catalysts could be manipulated by adjusting electronic and steric properties of ligands.<sup>18–20,30</sup> It has been shown that even a subtle change in the ligand structure might result in a drastically different reactivity. Recently, modification of the sidearm in organometallic catalysts has been proved to be an effective strategy for controlling the reactivity of transition

State Key Laboratory of Supramolecular Structure and Materials, College of Chemistry, Jilin University, Changchun, Jilin 130012, China.

E-mail: ytzhang2009@jlu.edu.cn

† Electronic supplementary information (ESI) available: Full experimental details, NMR spectra and additional polymerization data. See DOI: 10.1039/c8dt03941k

metal catalysts.<sup>31</sup> The catalytic properties of titanium complexes with monoanionic [N, X] (X = O, S, Se) ligands could be modulated by changing heteroatoms and substituents.<sup>32</sup> Similar sidearm effects have also been reported for Ni,<sup>33,34</sup> Cr<sup>35</sup> and other metal-based catalyst systems.<sup>34–38</sup> Moreover, sidearms with different chiral substituents have been applied in the asymmetric catalysis,<sup>39</sup> stereoselective ATRP of MMA<sup>40</sup> and isoselective ROP of *rac*-LA.<sup>41</sup> On the other hand, metal complexes containing a phenoxylimine ligand exhibited high reactivity for the polymerization of olefins.<sup>42–45</sup> Among which, aluminum alkyl complexes are of particular interest due to their low toxicity and high Lewis acidity and have already demonstrated that the sidearm structure plays an important role not only in polymerization of ethylene,<sup>46</sup> but also in ROP of lactones.<sup>47–56</sup> However, to the best of our knowledge, there has been no report about sidearm effects of aluminum alkyl complexes on the inhibition of transesterification during ROP of lactones so far.

In this contribution, five ligands, 2,4-di-*tert*-butyl-(dimethyl-amino)phenols with different C6-substituents, were prepared and employed for the synthesis of the corresponding dimethyl-aluminum complexes bearing with different sidearms, which achieved living ROP and copolymerization of lactones such as  $\epsilon$ -CL and  $\delta$ -VL in the presence of BnOH, producing well-defined (co)polymers with predicted MW, narrow MWD, and high initiation efficiency. Polymerization mechanistic studies as well as systematic investigations towards sidearm effects of catalysts on both polymerization activity and inhibition of transesterification were included in this study.

## Experimental

### Materials, reagents, and methods

All syntheses and manipulations of air- and moisture-sensitive materials were carried out in flamed Schlenk-type glassware on a dual-manifold Schlenk line, a high-vacuum line, or an argon-filled glovebox. Toluene and benzene were refluxed over a sodium/potassium alloy, followed by distillation under a nitrogen atmosphere; hexane and dichloromethane were refluxed over CaH<sub>2</sub>, followed by distillation under a nitrogen atmosphere. All solvents were stored over 4 Å molecular sieves. NMR spectra were recorded on a Varian Inova 300 (300 MHz, <sup>1</sup>H) or a Bruker Avance II 500 (500 MHz, <sup>1</sup>H; 126 MHz, <sup>13</sup>C) instrument at RT. Chemical shifts for <sup>1</sup>H and <sup>13</sup>C spectra were referenced to internal solvent resonances and are reported as parts per million relative to SiMe<sub>4</sub>. Air sensitive NMR samples were stored in Teflon-valve sealed J. Young-type NMR tubes.

Trimethylaluminum, triisobutylaluminum, 2,6-di-*tert*-butyl-4-methylphenol and paraformaldehyde were purchased from J&K. THF (HPLC grade) was purchased from Sigma. Diethylamine, 2-(methyl-amino)pyridine, *N,N,N'*-trimethylethylenediamine, hydrobromic acid, 2,4-di-*tert*-butylphenol, 3,5-di-*tert*-butyl-2-hydroxybenzaldehyde, *N*-methylbutan-1-amine, 8-aminoquinoline and 2,4,6-trimethylaniline were purchased from Energy Chemical. All chemicals were used as received unless otherwise specified as follows.  $\epsilon$ -Caprolactone

( $\epsilon$ -CL, J&K) and  $\delta$ -valerolactone ( $\delta$ -VL, Adamas-beta®) were dried over CaH<sub>2</sub>, distilled under nitrogen, and stored in a glovebox at –35 °C. Ligands **L1–L5** were prepared according to the modified literature procedures through the Mannich condensation reaction<sup>57,58</sup> or imine condensation reaction.<sup>59</sup> The detailed synthesis of **Al1–Al5** can be found in the ESI.†<sup>57–59</sup>

### General polymerization procedures

Polymerizations were performed either in 25 mL flame-dried Schlenk flasks interfaced to the dual-manifold Schlenk line for runs using an external temperature bath, or in 30 mL glass reactors inside the glovebox for runs carried out at rt. In a typical polymerization procedure in the presence of BnOH, a predetermined amount of **Al** complex solution and ROH were first mixed in toluene for 2 min, and 200 equiv. monomer (456  $\mu$ L for  $\delta$ -VL or 529  $\mu$ L for  $\epsilon$ -CL) was added to the mixture inside a glovebox. In a typical polymerization procedure in the absence of BnOH, a predetermined amount of **Al** complex solution was added into toluene, and the polymerization was started by rapid addition of a solution of monomer after two minutes. The amount of the monomer was fixed for all polymerizations. After the measured time interval, a 0.2 mL aliquot was taken from the reaction mixture *via* a syringe and quickly quenched into a 4 mL vial containing 0.6 mL of undried “wet” CDCl<sub>3</sub> stabilized by 250 ppm of BHT-H; the quenched aliquots were later analyzed by <sup>1</sup>H NMR to obtain the monomer conversion. After the polymerization was stirred for the stated reaction time, and the polymer was immediately precipitated by using 200 mL of hexane, stirred for 1 h, filtered, washed with hexane, and dried in a vacuum oven at 50 °C overnight to a constant weight.

### Polymerization kinetics

Kinetic experiments were carried out in a stirred glass reactor at ambient temperature (*ca.* 25 °C) inside an argon-filled glovebox using the polymerization procedure already described above, with an [Al3]/[BnOH]/[ $\epsilon$ -CL]<sub>0</sub> ratio of 1/1/800, 1/1/400, 1/1/200, and 1/1/100; [ $\epsilon$ -CL]<sub>0</sub> was fixed at 1.0 M. At appropriate time intervals, 0.2 mL aliquots were withdrawn from the reaction mixture using a syringe and quickly quenched into 4 mL septum-sealed vials containing 0.6 mL of undried “wet” CDCl<sub>3</sub> mixed with 250 ppm BHT-H. The quenched aliquots were analyzed by <sup>1</sup>H NMR for determining the ratio of [ $\epsilon$ -CL]<sub>*t*</sub> at a given time *t* to [ $\epsilon$ -CL]<sub>0</sub>, [ $\epsilon$ -CL]<sub>*t*</sub>: [ $\epsilon$ -CL]<sub>0</sub>. Apparent rate constants (*k*<sub>app</sub>) were extracted from the slopes of the best fit lines to the plots of ln([ $\epsilon$ -CL]<sub>0</sub>/[ $\epsilon$ -CL]<sub>*t*</sub>) *vs.* time. Another set of kinetic experiments were carried out with an [Al3]/[BnOH] ratio of 2/1, 4/1, 8/1, [ $\epsilon$ -CL]<sub>0</sub> was fixed at 1.0 M and [BnOH]<sub>0</sub> was fixed at 1.25 mM. For the third set of kinetic experiments carried out with an [Al3]/[BnOH] ratio of 1/2, 1/4, 1/8, [ $\epsilon$ -CL]<sub>0</sub> was fixed at 1.0 M and [Al3] was fixed at 1.25 mM. The rest of the procedure was the same as that described above.

### Polymer characterization

Gel permeation chromatography (GPC) analyses were performed on a Waters 1515 instrument equipped with a guard

column MIXED 7.5 × 50 mm PL column and two MIXED-C 7.5 × 300 columns and a differential refractive index detector using THF (HPLC grade) as the eluent at 35 °C with a flow rate of 1 mL min<sup>-1</sup>. The weight-average molar masses ( $M_w$ ) and MWD ( $M_w/M_n$ ) of the polymer samples were determined by WYATT DAWAN 8+. The differential refractive index (DRI) increment ( $dn/dc$ ) value of 0.084 mL g<sup>-1</sup> was used for PVL and 0.076 for PCL. Chromatograms were processed with Waters Breeze2 software.

The isolated low MW polymer samples were analyzed by matrix-assisted laser desorption/ionization time-of-flight mass spectroscopy (MALDI-TOF MS); the experiment was performed on a Bruker Autoflex III mass spectrometer in a linear, positive ion mode. The matrix was *trans*-2-[3-(4-*tert*-butylphenyl)-2-methyl-2-propylidene]malonitrile (DCTB), and the solvent was THF.

## Results and discussion

### Homopolymerization of $\epsilon$ -CL or $\delta$ -VL

Five ligands **L1–L5** (Fig. 1) having a similar chelating ring size and different substituents on N atoms were prepared according to the modified literature procedures through the Mannich condensation reaction<sup>57,58</sup> or imine condensation reaction.<sup>59</sup> The reaction of **L1–L5** with AlMe<sub>3</sub> at -35 °C afforded the corresponding dimethyl complexes **Al1–Al5** (Fig. 1). Control experiments indicated that ROP of  $\epsilon$ -CL or  $\delta$ -VL catalyzed by **Al1–Al5** alone in toluene all exhibited uncontrolled polymerization activity at RT and low initiation efficiencies ( $I^* < 29$ ) (Table S1†). It is reported that aluminum alkoxides *in situ* generated from the reaction of aluminum alkyls and alcohols can

initiate ROP of lactones.<sup>18,20,60</sup> Therefore, the initiator effect of the BnOH was examined for **Al1–Al5**-catalyzed ROP of  $\epsilon$ -CL or  $\delta$ -VL and representative polymerization results are summarized in Table 1. Gratifyingly, these **Al**/BnOH catalyst systems exhibited significantly enhanced polymerization activity for ROP of lactones, yielding polymers with controlled  $M_w$  and narrow MWD ( $D$  values as low as 1.12). With the increase of the  $\epsilon$ -CL-to-BnOH ratio from 200, 400 to 800, the  $M_w$  value of PCL produced by **Al1**/BnOH increased linearly from 40.4, 74.9 to 133 kg mol<sup>-1</sup>, while the  $D$  value remained in a narrow range of 1.51–1.53 and initiation efficiencies were kept around 85–105% (runs 1–3, Table 1).

As shown in Table 1, **Al2**/BnOH exhibited the fastest polymerization activity for ROP of  $\epsilon$ -CL among the investigated **Al**/BnOH catalyst systems. With a 400:1 [ $\epsilon$ -CL]:[**Al**] ratio, it only took the **Al2**/BnOH system 1.25 h to reach a 97.0% conversion of  $\epsilon$ -CL (run 5, Table 1), whereas it took 2.5 h for **Al1**/BnOH (run 2, Table 1), 3.6 h for **Al3**/BnOH (run 9, Table 1) and 20 h for **Al4**/BnOH (run 13, Table 1) to reach high to near quantitative conversion of  $\epsilon$ -CL. Due to its high polymerization activity, the **Al2**/BnOH system could obtain a 98.2% monomer conversion even with a 2000:1 [ $\epsilon$ -CL]:[**Al2**] ratio within 10 h and produce the polymer with  $M_w = 303$  kg mol<sup>-1</sup> and a narrow  $D$  value of 1.44 (run 7, Table 1), thus giving rise to an initiation efficiency ( $I^*$ ) of 106. Replacing **Al2** with **Al3** possessing one more *N*-methyl group could polymerize 92% of 1600 equiv.  $\epsilon$ -CL into PCL with  $M_w = 173$  kg mol<sup>-1</sup> and  $D = 1.57$  in 7.5 h (run 11, Table 1).  $I^*$  of 153 indicated that there exists chain transfer under this condition. Switching to **Al4** having a pyridine substituent on the sidearm, a 98% conversion of 800 equiv.  $\epsilon$ -CL was obtained in 24 h, producing PCL with  $M_w = 115$  kg mol<sup>-1</sup>,  $D = 1.46$  and  $I^* = 114$  (run 14,

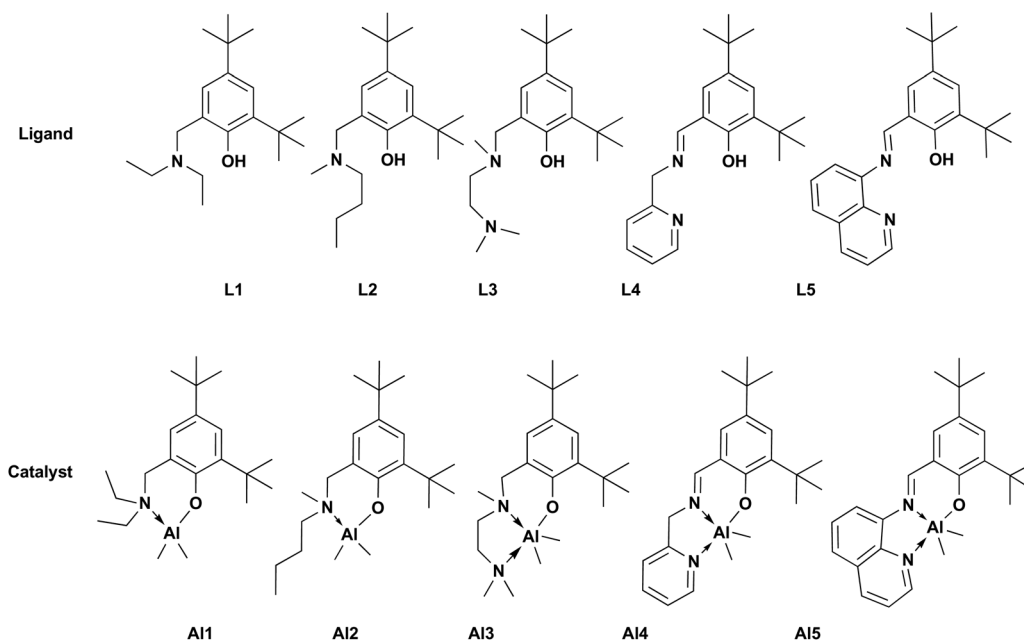


Fig. 1 Structures of **L1–L5** and **Al1–Al5**.

Table 1 Selected polymerization results by the Al1–Al5/BnOH catalyst system<sup>a</sup>

Run	Al	M/Al	Al/BnOH	Time (h)	Conv. <sup>b</sup> (%)	$M_n^c$ (kg mol <sup>-1</sup> )	$M_w^c$ (kg mol <sup>-1</sup> )	$\mathcal{D}$	$I^*^d$ (%)
1	Al1	200CL	1 : 1	1.5	100.0	26.8	40.4	1.51	85
2	Al1	400CL	1 : 1	2.5	96.3	49.1	74.9	1.53	90
3	Al1	800CL	1 : 1	6.0	100.0	87.4	133	1.52	105
4	Al2	200CL	1 : 1	1.0	100.0	25.2	37.8	1.50	91
5	Al2	400CL	1 : 1	1.25	97.0	46.8	69.2	1.48	95
6	Al2	800CL	1 : 1	2.5	97.0	85.1	126	1.48	104
7	Al2	2000CL	1 : 1	10.0	98.2	211	303	1.44	106
8	Al3	200CL	1 : 1	3.6	100.0	22.7	31.9	1.41	101
9	Al3	400CL	1 : 1	3.6	98.0	43.8	63.9	1.46	102
10	Al3	800CL	1 : 1	5.5	96.0	77.1	116	1.50	114
11	Al3	1600CL	1 : 1	7.5	92.0	101	173	1.57	153
12	Al4	200CL	1 : 1	9.5	100.0	25.2	36.9	1.46	90
13	Al4	400CL	1 : 1	20.0	99.0	45.0	68.8	1.53	100
14	Al4	800CL	1 : 1	24.0	98.0	78.5	115	1.46	114
15	Al5	200CL	1 : 1	14.5	76.1	76.3	119	1.56	23
16	Al1	200VL	1 : 1	1.5	93.5	20.7	30.4	1.47	90
17	Al2	200VL	1 : 1	1.5	93.7	19.1	27.6	1.45	99
18	Al3	200VL	1 : 1	1.5	93.6	15.9	26.1	1.64	118
19	Al4	200VL	1 : 1	11.0	93.6	17.4	26.0	1.49	108
20	Al5	200VL	1 : 1	14.5	47.3	64.7	89.6	1.38	15

<sup>a</sup> Condition: Carried out at ambient temperature (~25 °C) in toluene,  $[M]_0 = [\text{monomer}] = 1.0 \text{ M}$ . <sup>b</sup> Monomer conversions measured by <sup>1</sup>H NMR. <sup>c</sup> Absolute molecular weight ( $M_w$ ) measured by GPC using a light scattering detector. Number average molecular weight ( $M_n$ ) is calculated from  $M_w/\mathcal{D}$ . <sup>d</sup> Initiation efficiency ( $I^*$ )% =  $M_n(\text{calcd})/M_n(\text{exptl}) \times 100$ , where  $M_n(\text{calcd}) = \text{MW}(\text{M}) \times ([M]/[I]) \times (\text{conversion}) + \text{MW of chain-end groups}$ .

Table 1). It should be noted that Al5 possessing a bulky chelating N-containing substituent showed drastically decreased polymerization activity and poor control on the ROP of  $\epsilon$ -CL. It took 14.5 h to convert 76.1% of 200 equiv.  $\epsilon$ -CL to PCL with  $M_w = 119 \text{ kg mol}^{-1}$ ,  $\mathcal{D} = 1.56$  and a relatively low  $I^*\% = 23$  (run 15, Table 1). Switching from  $\epsilon$ -CL to  $\delta$ -VL, all Al1–Al4/BnOH catalyst systems are effective for polymerization with a 200 : 1 [ $\delta$ -VL]:[Al] ratio and achieved high to near quantitative monomer conversion, affording PVL with  $M_w = 26.0$ – $30.4 \text{ kg mol}^{-1}$ ,  $\mathcal{D} = 1.45$ – $1.64$  and near quantitative initiation efficiencies (runs 16–19, Table 1). For Al5/BnOH, only 47.3% monomer conversion could be obtained in 14.5 h, furnishing PVL with high  $M_w = 119 \text{ kg mol}^{-1}$ ,  $\mathcal{D} = 1.45$ , and thus giving rise to a low initiation efficiency  $I^*\%$  of 15 (run 20, Table 1).

As can be seen from the above-mentioned results, a similar polymerization activity trend was observed for ROP of both  $\delta$ -VL and  $\epsilon$ -CL by these Al/BnOH systems, following the order of Al2 > Al1 > Al3 > Al4 > Al5. More specifically, Al2/BnOH showed the highest polymerization activity, while Al5/BnOH had the lowest one. These results indicated that the N-containing substituent on the sidearm of the Al-based catalysts plays an important key role in the reactivity of ROP. As shown in <sup>1</sup>H NMR spectra, chemical shifts assigned for the AlCH<sub>3</sub> group in Al1–Al5 are  $-0.41$  (Al1),  $-0.43$  (Al2),  $-0.40$  (Al3),  $-0.17$  (Al4) and  $-0.05$  (Al5), respectively (Fig. S11†). The chemical shift order of Al2 < Al1 < Al3 < Al4 < Al5 revealed that Lewis acidity of Al1 to Al5 is also decreased in the same order such that Al2 possesses the smallest Lewis acidity, while Al5 has the largest one. This is in contrast to the polymerization activity trend, which means during polymerization, the smallest Lewis acidity enabled Al2 to exhibit the easiest cleavage of the Al–O(Bn) bond and the subsequent nucleophilic attack of

carbonyl carbon of the activated monomer by the BnO-group, thus leading to the fastest insertion to lactones.<sup>61</sup> *Vice versa*, Al5 with the largest Lewis acidity exhibited the lowest polymerization activity. Moreover, it should be noted that we observed a doublet signal assigned for AlCH<sub>3</sub> for Al2, whereas only a single peak for Al1, suggesting effects of the different sidearms in Al1–Al5 on the Al center. For Al3, Al4, and Al5 having more than one N-containing substituents on the sidearm, the possibility that the N atom could be reversibly coordinated to the central Al atom imposed an important impact on interaction between the catalyst and benzyl alcohol or monomers, thereby leading to different polymerization activity. The poor control and lower polymerization activity of Al5 might be ascribed to the steric hindrance of the larger sidearm.

#### Living ROP of $\epsilon$ -CL by Al/BnOH

The above results showed that Al1–Al4/BnOH systems all possessed a high degree of control over ROP of  $\epsilon$ -CL; we further interrogated the living features of polymerization. First, varying the  $[CL]_0/[Al2]_0/[BnOH]_0$  ratio from 200 : 1 : 1 to 2000 : 1 : 1 achieved high to near quantitative monomer conversion for all ratios and produced PCL with controlled MWs, low  $\mathcal{D}$  values (1.44–1.50), and high initiation efficiencies (91–106%, run 4–7, Table 1). It is worth noting that in the presence of BnOH, Al1, Al3 and Al4 also exhibited similar polymerization performance (Table 1). Second, GPC traces of PCL samples produced by Al/BnOH showed a gradual shift to the higher-molar-mass region with an increase in the  $[\epsilon\text{-CL}]_0/[BnOH]_0$  ratio while maintaining a narrow and unimodal MWD (Fig. S20†). Third, the  $M_n$  value of PCL produced by Al2/BnOH increased linearly ( $R^2 = 0.999$ ) with an increase in the  $[\epsilon\text{-CL}]_0/[Al2]_0/[BnOH]_0$  ratio from 200 : 1 : 1 to 2000 : 1 : 1, while the  $\mathcal{D}$  value

remained in a narrow range between 1.44 and 1.50 (Fig. S13a†). It should be noted that similar features were also observed for **Al1** ( $R^2 = 0.999$ ), **Al3** ( $R^2 = 0.996$ ), and **Al4** ( $R^2 = 0.993$ ) in the presence of BnOH (Fig. S13b†). Fourth, A straight line was obtained for the plot of the PCL  $M_n$  vs. monomer conversion at a fixed  $[\epsilon\text{-CL}]_0/[\mathbf{3}]_0/[\text{BnOH}]_0$  ratio of 800 : 1 : 1 ( $R^2 = 0.962$ , Fig. S18a†) and at a  $[\epsilon\text{-CL}]_0/[\mathbf{4}]_0/[\text{BnOH}]_0$  ratio of 200 : 1 : 1 ( $R^2 = 0.979$ , Fig. S18b†), respectively, which were both coupled with small  $D$  values. Fifth, both chain extension and copolymerization (*vide infra*) experiments provided more direct evidence for living characteristics of polymerization. PCL with  $M_w = 36.9 \text{ kg mol}^{-1}$  and  $D = 1.46$  was first prepared by polymerizing 200 equiv. of  $\epsilon\text{-CL}$  to completion without quenching. The polymerization was resumed by addition of another 200 equiv. of  $\epsilon\text{-CL}$ , affording the resulting PCL with  $M_w = 70.0 \text{ kg mol}^{-1}$  and  $D = 1.46$  (run 1, Table 2).

To gain more insights into the polymerization mechanism, we investigated the kinetics of ROP of  $\epsilon\text{-CL}$  by **Al3**/BnOH employing a fixed  $[\mathbf{Al3}]_0/[\text{BnOH}]_0$  ratio of 1 : 1 but varied  $[\epsilon\text{-CL}]_0/[\mathbf{Al3}]_0/[\text{BnOH}]_0$  ratio:  $[\epsilon\text{-CL}]_0/[\mathbf{Al3}]_0/[\text{BnOH}]_0$  ratio = 100 : 1 : 1, 200 : 1 : 1, 400 : 1 : 1, and 800 : 1 : 1. As can be seen from the representative kinetic plots of  $\ln([\epsilon\text{-CL}]_0/[\epsilon\text{-CL}]_t)$  vs. time (Fig. 2), the polymerization clearly showed no induction period and a strict first-order with respect to  $[\epsilon\text{-CL}]$  concentration for all ratios examined herein.<sup>62–64</sup> Since the  $[\mathbf{Al3}]/[\text{BnOH}]$  ratio was kept at 1, the combined kinetic order of  $[\mathbf{Al3}]$  and  $[\text{BnOH}]$  can be obtained from the double logarithm plot of the apparent rate constants ( $K_{\text{app}}$ ) obtained from the slopes of the best-fit lines to the plots of  $\ln([\epsilon\text{-CL}]_0/[\epsilon\text{-CL}]_t)$  vs. time as a function of  $\ln[\mathbf{Al3}]$ , which was fit to a straight line ( $R^2 = 0.997$ ) with a slope of 0.938. Thus, these results revealed that the combined kinetics order of **Al3** and BnOH is 1.<sup>64</sup> In the second set of kinetic experiments, the  $[\epsilon\text{-CL}]_0/[\mathbf{Al3}]_0$  ratio was fixed to be 800 : 1, while  $[\text{BnOH}]$  was varied with a  $[\epsilon\text{-CL}]_0/[\mathbf{Al3}]_0/[\text{BnOH}]_0$  ratio of 800 : 1 : 2, 800 : 1 : 4, and 800 : 1 : 8. As shown in Fig. 3a, the same first-order dependence on monomer concentration was observed for all ratios investigated in this study and polymerization with a 800 : 1 : 2

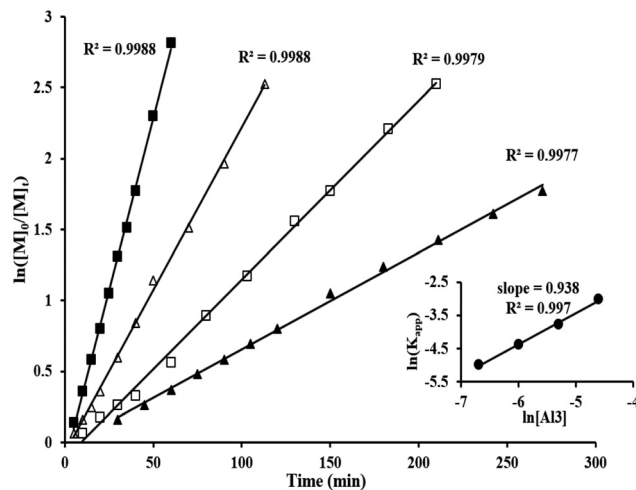


**Fig. 2** First-order kinetic plots for ROP of  $\epsilon\text{-CL}$  by **Al3**/BnOH in toluene at RT:  $[\epsilon\text{-CL}]_0 = 1.0 \text{ M}$ ;  $[\text{BnOH}]_0 = [\mathbf{Al3}]_0$ ;  $[\mathbf{Al3}]_0 = 0.01 \text{ M}$  (■),  $0.005 \text{ M}$  (Δ),  $0.0025 \text{ M}$  (□),  $0.00125 \text{ M}$  (▲). Inset: plot of  $\ln(K_{\text{app}})$  vs.  $\ln[\mathbf{Al3}]$ .

$[\epsilon\text{-CL}]_0/[\mathbf{Al3}]_0/[\text{BnOH}]_0$  ratio is far more effective than polymerization with a 800 : 1 : 1 ratio, but further increasing the ratio of  $[\text{BnOH}]_0/[\mathbf{Al3}]_0$  from 2 to 4 and 8 did not result in the enhancement of the polymerization rate. In the third set of kinetic experiments, the  $[\epsilon\text{-CL}]_0/[\text{BnOH}]_0$  ratio was fixed to be 800, while the  $[\mathbf{Al3}]$  was varied:  $[\epsilon\text{-CL}]_0/[\mathbf{Al3}]_0/[\text{BnOH}]_0$  ratio of 800 : 1 : 1, 800 : 2 : 1, 800 : 4 : 1 and 800 : 8 : 1. Besides the same first-order dependence on monomer concentration was observed for all ratios; the polymerization rate was decreased with an increase in  $[\mathbf{Al3}]$  concentration (Fig. 3b). The above-mentioned results combined with chain-end analysis results obtained from MALDI-TOF-MS measurements (*vide infra*) clearly rule out the monomer-activated mechanism<sup>4,65,66</sup> and a coordination–insertion mechanism<sup>4,64</sup> was proposed as shown in Scheme 1.  $\text{LAlMe}_2$  reacted with BnOH to form the real catalysts either  $\text{LAlMeOBn}$  (path a) or  $\text{LAl}(\text{OBn})_2$  (path b) depending on the amount of  $[\text{BnOH}]$ , which could be confirmed by

**Table 2** Copolymerization of  $\epsilon\text{-CL}$  and  $\delta\text{-VL}$  catalyzed by **Al1–Al4**/BnOH<sup>a</sup>

Run	Al	M1/M2	Al/BnOH	Conv. <sup>b</sup> (%)	$M_n$ <sup>c</sup> (kg mol <sup>-1</sup> )	$M_w$ <sup>c</sup> (kg mol <sup>-1</sup> )	$D$
1	<b>Al4</b>	200CL/200CL	1 : 1	CL: 100	48.1	70.0	1.46
2 <sup>d</sup>	<b>Al4</b>	200CL and 200VL	1 : 1	CL: 100 VL: 99	61.9	75.9	1.26
3	<b>Al4</b>	200CL/200VL	1 : 1	CL: 100 VL: 95	44.0	66.4	1.51
4	<b>Al4</b>	200CL/200VL/200CL	1 : 1	CL: 76 VL: 100	61.3	91.9	1.50
5	<b>Al1</b>	200CL/200VL	1 : 1	CL: 100 VL: 98	39.1	58.8	1.50
6	<b>Al2</b>	200CL/200VL	1 : 1	CL: 100 VL: 97	38.0	57.5	1.52
7	<b>Al3</b>	200CL/200VL	1 : 1	CL: 100 VL: 98	33.6	53.9	1.60

<sup>a</sup> Carried out at ambient temperature ( $\sim 25 \text{ }^\circ\text{C}$ ) in toluene, where  $[\text{M}]_0 = 1.0 \text{ M}$ . <sup>b</sup> Monomer conversions measured by  $^1\text{H NMR}$ . <sup>c</sup> Absolute molecular weight ( $M_w$ ) measured by GPC using a light scattering detector. Number average molecular weight ( $M_n$ ) is calculated from  $M_w/D$ . <sup>d</sup> Both monomers were added at the same time.

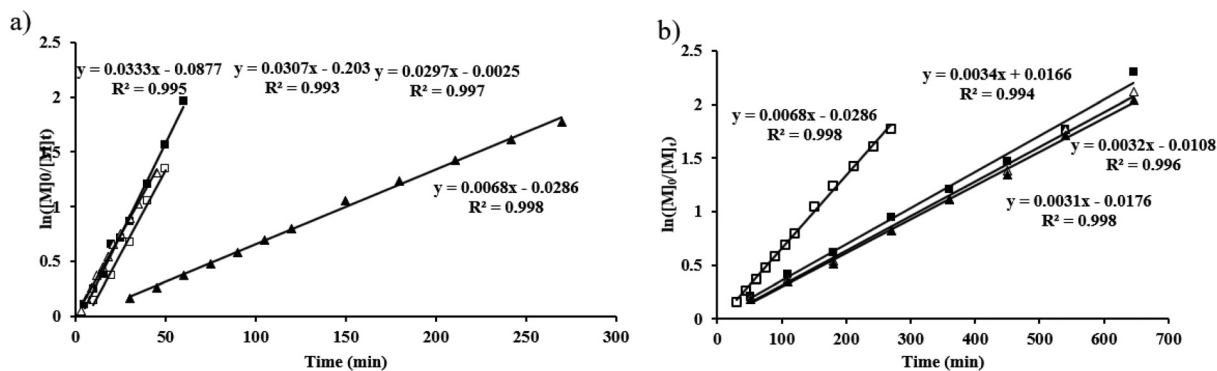
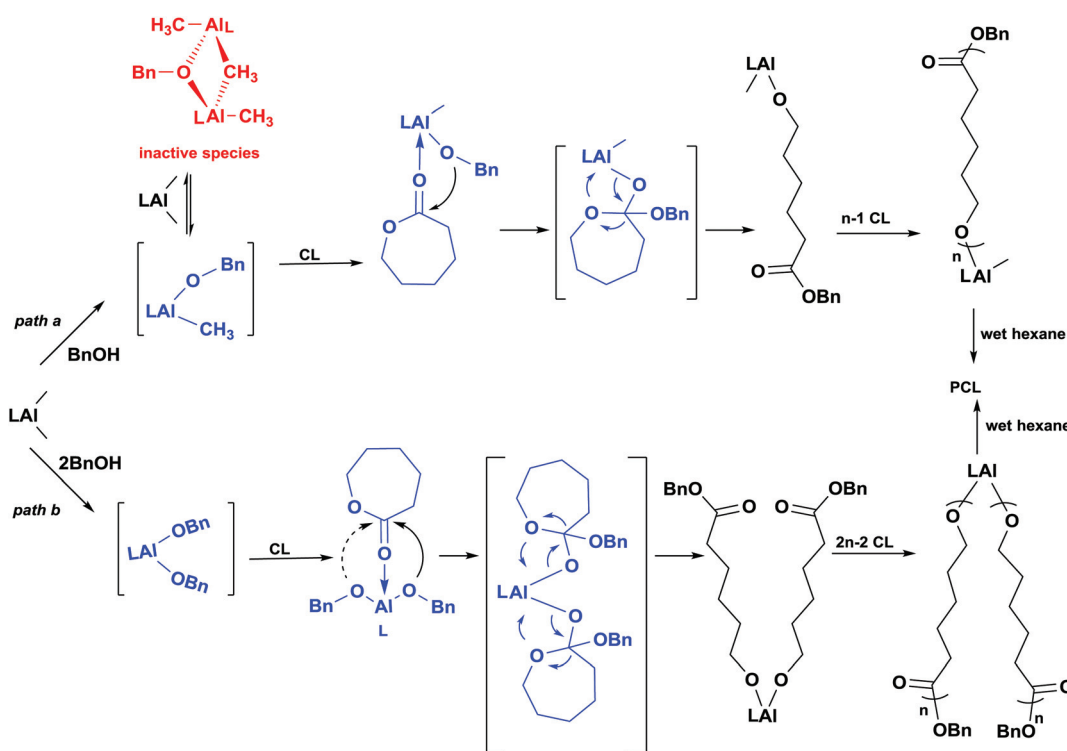


Fig. 3 Kinetic plots for  $Al_3/BnOH$ -catalyzed ROP of  $\epsilon$ -CL under the condition of  $[e-CL]_0 = 1.0$  M in toluene at RT; (a)  $[Al_3]_0$  was fixed at 0.00125 M,  $[BnOH]_0 = 0.005$  M ( $\blacksquare$ ), 0.0025 M ( $\triangle$ ), 0.01 M ( $\square$ ), 0.00125 M ( $\blacktriangle$ ); (b)  $[BnOH]_0$  was fixed at 0.00125 M,  $[Al_3]_0 = 0.00125$  M ( $\square$ ), 0.0025 M ( $\blacksquare$ ), 0.005 M ( $\triangle$ ), 0.01 M ( $\blacktriangle$ ).



Scheme 1 A plausible coordination–insertion mechanism for ROP of  $\epsilon$ -CL by the  $Al/BnOH$  catalyst system.

observance of  $CH_4$  at 0.15 ppm in the  $^1H$  NMR spectrum obtained from the reaction of  $Al_3$  and  $BnOH$  (Fig. S19<sup>†</sup>). It should be noted that the  $^1H$  NMR spectrum is quite complicated and products are unstable in the absence of monomers. In the presence of the monomers, nucleophilic attack of carbonyl carbon of the activated monomer by the  $BnO$ -group initiates polymerization *via* a coordination–insertion mechanism (path a). When the ratio of  $[BnOH]_0/[Al_3]_0$  is increased from 1 to 2 (path b), the polymerization rate was drastically enhanced since the *in situ* generated active species  $LAl(OBn)_2$  could serve as an intramolecular bis-initiator to initiate two polymer chains at the same time. However, comparable

polymerization activity was observed for polymerization with a  $[BnOH]_0/[Al_3]_0$  ratio over 2 (Fig. 3a). These results provided more supporting evidence for the coordination–insertion reaction mechanism since the polymerization rate did not increase with the increase of  $[BnOH]_0$  concentration after the  $[BnOH]_0/[Al_3]_0$  ratio is  $>2$  where it should be enhanced with the increase of both  $[BnOH]$  and  $[Al_3]$  concentration if it was a monomer-activation mechanism. The excess  $BnOH$  could serve as a chain transfer agent to exchange with the living chain ends  $Al-O$  to form new active chain ends, thus leading to the decrease of  $M_w$  of the polymer and increase of initiation efficiencies. As shown in Table S3,<sup>†</sup> for polymerization with a

fixed 800 : 1  $[\epsilon\text{-CL}]_0/[\text{Al3}]_0$  ratio, an increase of BnOH from 1 equiv. to 2, 3, 5 and 10 equiv. resulted in the decrease of  $M_w$  of the polymer from 116  $\text{kg mol}^{-1}$  to 49.7, 36.6, 18.1 and 8.5  $\text{kg mol}^{-1}$ , thus achieving the increase of initiation efficiencies from 114 to 267, 355, 595 and 1142, respectively. GPC traces of these produced PCL samples showed the corresponding gradual shift to the lower-molar-mass region (Fig. S12<sup>†</sup>). On the other hand, the excess  $\text{LAlMe}_2$  did not increase but decrease the polymerization rate, which further confirmed the coordination insertion mechanism rather than the monomer-activation mechanism. The fact that only 2.4% of monomer conversion was obtained for the control experiment with a 1 : 800  $[\text{Al3}]_0/[\epsilon\text{-CL}]_0$  ratio in 24 h suggested the negligible effect of **Al3** itself for polymerization. The above-mentioned results indicated that excess **Al3** might react with real catalysts  $\text{LAlMeOBn}$  to generate *inactive species* for polymerization (Scheme 1),<sup>64</sup> thus leading to the decrease of the polymerization rate (Fig. 3b). It should be noted that all polymerizations with a fixed 800 : 1  $[\epsilon\text{-CL}]_0/[\text{BnOH}]_0$  ratio but varied  $[\text{Al3}]_0$  concentration produced polymers with similar  $M_w$  and MWD values (Table S2<sup>†</sup>), which indicated that such *inactive species* could be reversibly dissociated to release  $\text{LAlMeOBn}$  for the initiation of polymerization.

#### Copolymerization of $\epsilon\text{-CL}$ and $\delta\text{-VL}$ catalyzed by the **Al1–Al4/BnOH** system

As the major drawback in the application of the copolyester obtained from ROP of lactones, the transesterification side reaction including inter- and intramolecular transesterification

always led to random copolymers with broad dispersities,<sup>21–27</sup> and thus it is difficult to achieve multiblock copolymers or sequence-controlled block copolymers. Previously, the employment of living ROP of lactones by N-heterocyclic olefin/ $\text{Al}(\text{C}_6\text{F}_5)_3$  Lewis pairs enabled us to successfully prepare well-defined multi-block copolymers without transesterification.<sup>29</sup> Therefore, the identification of living ROPs of both  $\epsilon\text{-CL}$  and  $\delta\text{-VL}$  catalyzed by the **Al1–Al4/BnOH** system prompted us to further apply these catalyst systems to the synthesis of multi-block copolymers. When both monomers were added at the same time, copolymerization of  $\epsilon\text{-CL}$  and  $\delta\text{-VL}$  produced random copolymers (run 2, Table 2), as quantitative  $^{13}\text{C}$  NMR spectra (Fig. S14<sup>†</sup>) showing the characteristic of a random copolymer that four equal integrals of each type of methylene resonance were observed within copolymer [VL–CL (0.23), CL–CL (0.28), VL–VL (0.23), CL–VL (0.26)]. To our great satisfaction, linear diblock copolymer PCL-*b*-PVL could be successfully obtained through the sequential block copolymerization method by polymerizing  $\epsilon\text{-CL}$  first with  $[\epsilon\text{-CL}]_0/[\text{Al4}]_0/[\text{BnOH}]_0 = 200/1/1$  without quenching, followed by addition of another 200 equiv.  $\delta\text{-VL}$  (run 3, Table 2). As shown in  $^{13}\text{C}$  NMR spectra (Fig. 4d), methylene signals assigned for copolymer PCL-*b*-PVL produced by **Al4/BnOH** exhibited two equal integrals corresponding to homodyads CL–CL and VL–VL without observance for heterodyads VL–CL and CL–VL, which implies that the **Al4/BnOH** system produced a well-defined diblock copolymer without occurrence of the transesterification side reaction under this condition. GPC traces provided further evidence for

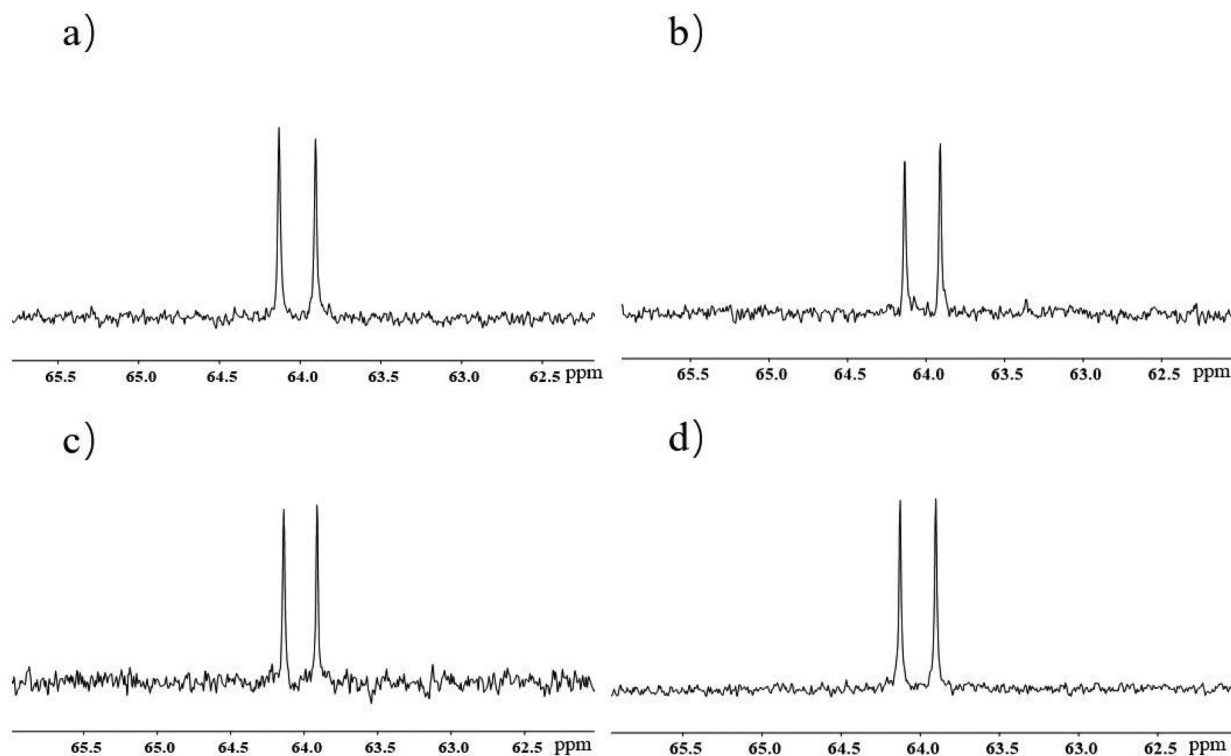


Fig. 4  $^{13}\text{C}$  NMR spectra of linear diblock PCL-*b*-PVL produced by (a) **Al1/BnOH**; (b) **Al2/BnOH**; (c) **Al3/BnOH**; (d) **Al4/BnOH** system at RT.

the formation of a well-defined block copolymer by **Al4**/BnOH systems in toluene at RT (Fig. S21d†). GPC traces for PCL produced during the first ROP shifted to a higher molecular weight region with a low dispersity value of  $D = 1.46$ – $1.51$ , while  $M_w$  values increased from  $36.9 \text{ kg mol}^{-1}$  for homopolymer PCL (black trace) to  $66.4 \text{ kg mol}^{-1}$  for diblock copolymer PCL-*b*-PVL (red trace). In addition, through this sequential monomer addition method, triblock copolymer PCL-*b*-PVL-*b*-PCL was also successfully prepared with an  $M_w$  value of  $91.9 \text{ kg mol}^{-1}$  (blue trace) and a  $D$  value of 1.50 (run 4, Table 2). When switching from **Al4** to the other **Al**-based catalyst, both  $^{13}\text{C}$  NMR spectra (Fig. 4a–c) and GPC traces (Fig. S21a–c†) clearly indicated that these **Al1**–**Al3**/BnOH catalyst systems are all capable of synthesizing the well-defined block copolymers (runs 5–7, Table 2). To the best of our knowledge, there is no such report that **Al**-based catalyst systems were employed for this purpose.

Although well-defined block copolymers could be prepared through the strict control over experimental conditions, such as reaction time and temperature, it would be more desirable to develop a robust catalyst to accomplish the goal without these restrictions. Therefore, in order to test whether these **Al**-based catalyst systems are robust enough for the synthesis of well-defined block copolymers, the copolymerization of  $\epsilon$ -CL and  $\delta$ -VL was carried out under prolonged reaction time or increased reaction temperature, since the transesterification side reaction more likely occurred under such conditions. It turned out that transesterification side reaction was observed for copolymerization catalyzed by **Al1**–**Al3**/BnOH catalyst systems with prolonged reaction time. As revealed by  $^{13}\text{C}$  NMR spectra (Fig. S15a–c†), new signals assigned for heterodyads VL–CL and CL–VL were observed in copolymers obtained after 10 h of complete monomer consumption at RT, while for the **Al4**/BnOH system, the block copolymer structure could be well-maintained at RT even after 24 h (Fig. S15d†). On the other hand, without quenching after complete monomer consumption is reached, the reaction mixture was heated at  $50 \text{ }^\circ\text{C}$  for 10 h and transesterification was observed for the copolymerization catalyzed by **Al1**–**3**/BnOH, producing random copolymers (Fig. S16a, b† and Fig. 5a), for the copolymer produced by

**Al3**/[BnOH], [VL–CL (0.13), CL–CL (0.38), VL–VL (0.34), CL–VL (0.15)] (Fig. 5a), whereas the **Al4**/BnOH system still produced the well-defined block copolymer even after heating at  $50 \text{ }^\circ\text{C}$  for 10 h (Fig. 5b). The aforementioned results indicated that different sidearms in **Al**-based catalysts might impose significant impacts on synthesizing and maintaining well-defined block copolymers in polymerization.

For copolymerization producing block copolymers under controlled reaction conditions, transesterification does not occur when the monomer was not completely consumed; otherwise, it occurs. This is to say that the monomer is more easily activated than the produced polymer chain in these cases. It is reported that LA could activate the ester group of the growing polymer chain and lead to the backbiting chain-termination process during polymerization of acrylic monomers catalyzed by Lewis pairs.<sup>67,68</sup> By choosing suitable LA with appropriate Lewis acidity and steric hindrance, the backbiting could be successfully suppressed, thus achieving living/controlled polymerization.<sup>69</sup> On the basis of the above-mentioned results, we believed that different sidearm structures of the ligand in these **Al**-based catalysts have significant important effects on the coordination ability of catalysts, which enabled them to only activate monomers with ring tension instead of polymeric chains, thus producing well-defined block polymers without requirement of strict-control over reaction conditions. More specifically, the **Al4** system with a pyridine group on the sidearm exhibited better performance on inhibition of transesterification, since the coordination of the rigid pyridine group with an aluminum centre might prevent its coordination with polymers after complete consumption of monomers, thus preventing transesterification and producing well-defined block copolymers (Fig. 5b), in contrast to the random copolymer produced by **Al3**-promoted polymerization heated at  $50 \text{ }^\circ\text{C}$  for 10 hours (Fig. 5a). The effects of different sidearms in **Al**-based catalysts imposed on the suppressing intramolecular transesterification side reaction could also be indirectly confirmed by chain-end analyses with MALDI-TOF MS measurement (*vide infra*).

The end-group of the low MW oligomers produced by **Al**/BnOH systems was analyzed by the matrix assisted laser de-

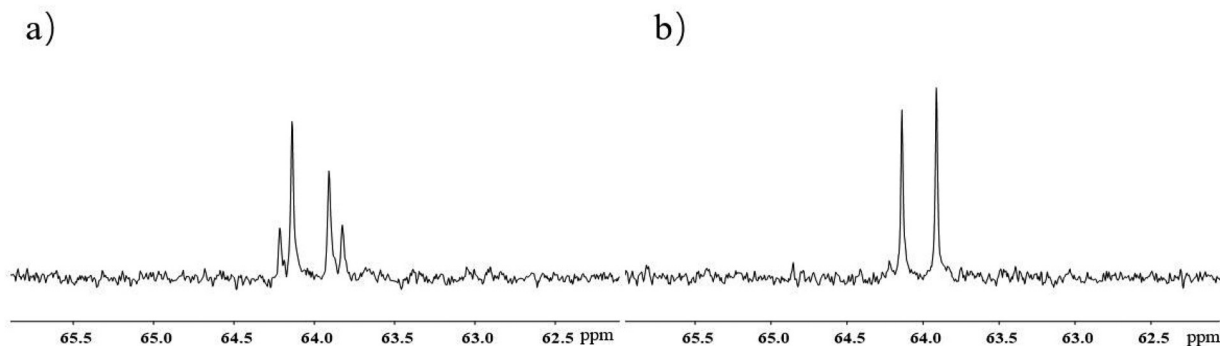


Fig. 5  $^{13}\text{C}$  NMR spectra of copolymers produced by (a) **Al3**/BnOH and (b) **Al4**/BnOH system heated at  $50 \text{ }^\circ\text{C}$  for 10 h after the monomer consumption.

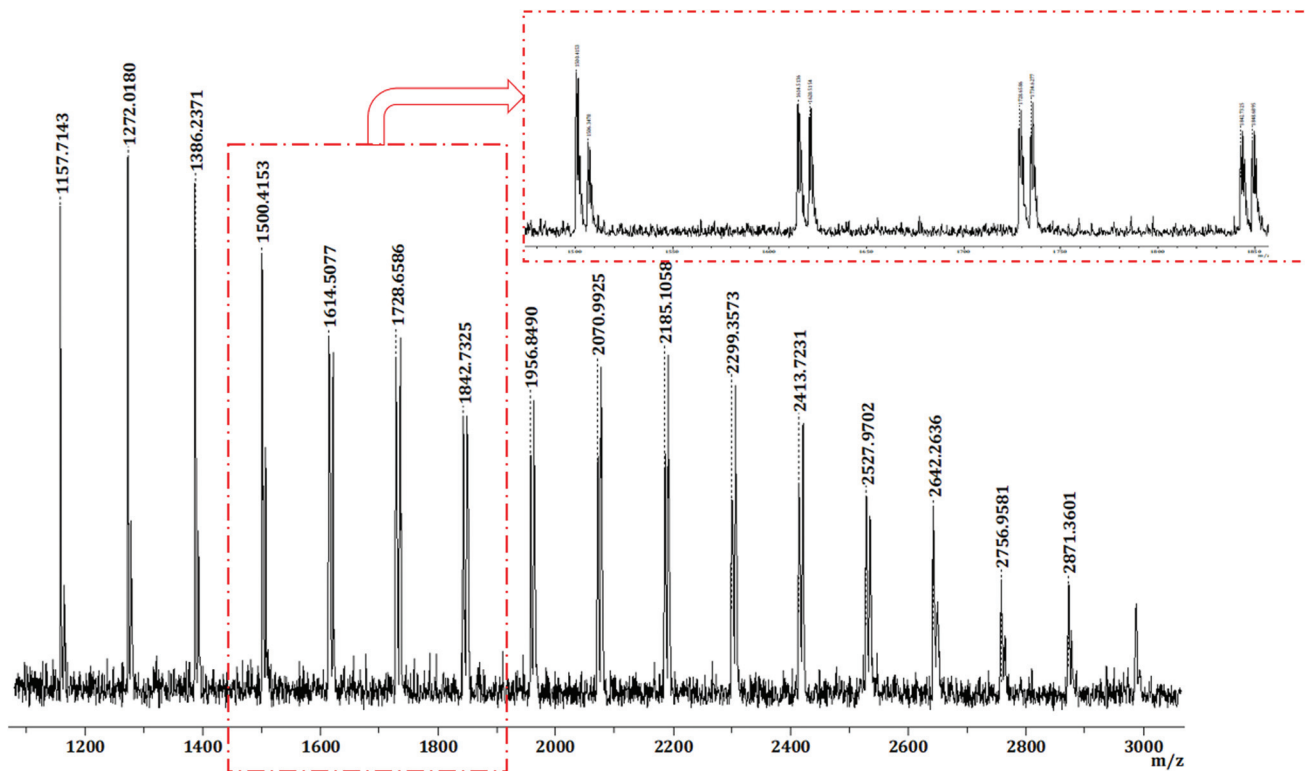


Fig. 6 The MALDI-TOF MS analysis of the resulting PCL produced by Al<sub>3</sub>/BnOH in toluene at RT.

sorption/ionization time-of-flight mass spectroscopy (MALDI-TOF MS). As it can be seen from Fig. 6, MS of PCL produced by the Al<sub>3</sub>/BnOH system consisted of two series of molecular mass ions. A plot of  $m/z$  values for the left series in the MS spectrum vs. the number of  $\epsilon$ -CL repeat units ( $n$ ) afforded a straight line with a slope of 114 and an intercept of 131 (Fig. 7a); the slope corresponds to the exact mass of the  $\epsilon$ -CL monomer, whereas the intercept is the sum of the end groups:  $n \epsilon$ -CL + BnOH + Na<sup>+</sup>. This analysis yielded a polymer chain with BnOH chain-ends. Furthermore, a linear plot of  $m/z$  values for the right series in the MS spectrum vs. the  $\epsilon$ -CL repeat units ( $n$ ) gave the same slope but a different intercept of 23 (Fig. 7b), which corresponds to the molecular mass of

sodium ions, indicating the formation of intramolecular cyclization products without chain-ends due to the intramolecular transesterification. In order to provide experimental evidence for the formation of the cyclic PCL polymer, we utilized GPC with a light scattering detector coupled to a viscometer to analyse and compare PCL1 (prepared after reaching monomer completion) and PCL2 (kept at RT for 24 h after reaching monomer completion) produced by the Al<sub>3</sub>/BnOH system. As shown in Fig. S17,<sup>†</sup> PCL2 exhibited slightly lower intrinsic viscosity (0.93) than PCL1, which indicated that PCL2 was composed of linear polymers and cyclic polymers resulting from intramolecular transesterification. On the other hand, broader  $D$  values which increased from 1.18 to 1.26 also suggested the

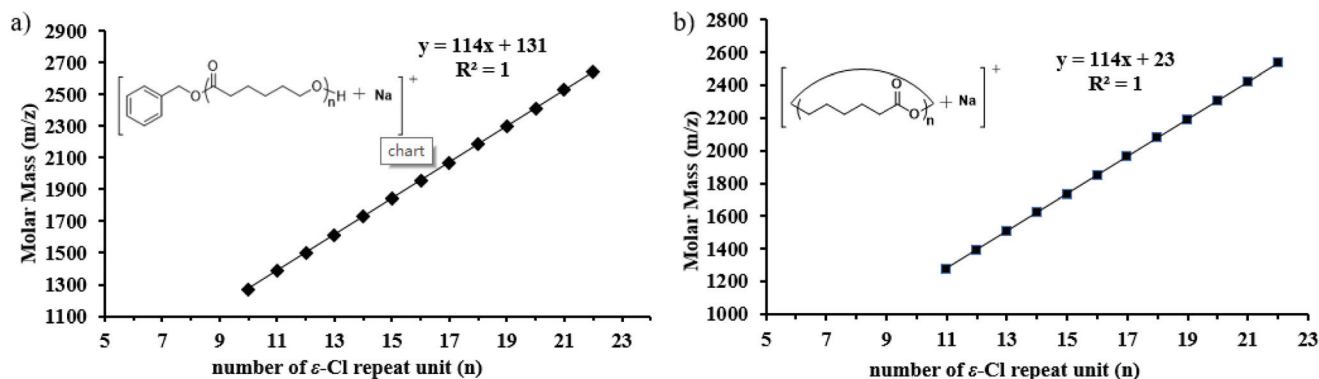


Fig. 7 Plot of  $m/z$  values from Fig. 6 vs. the number of  $\epsilon$ -CL repeat units ( $n$ ) for: (a) the major series (left) and (b) minor series (right).

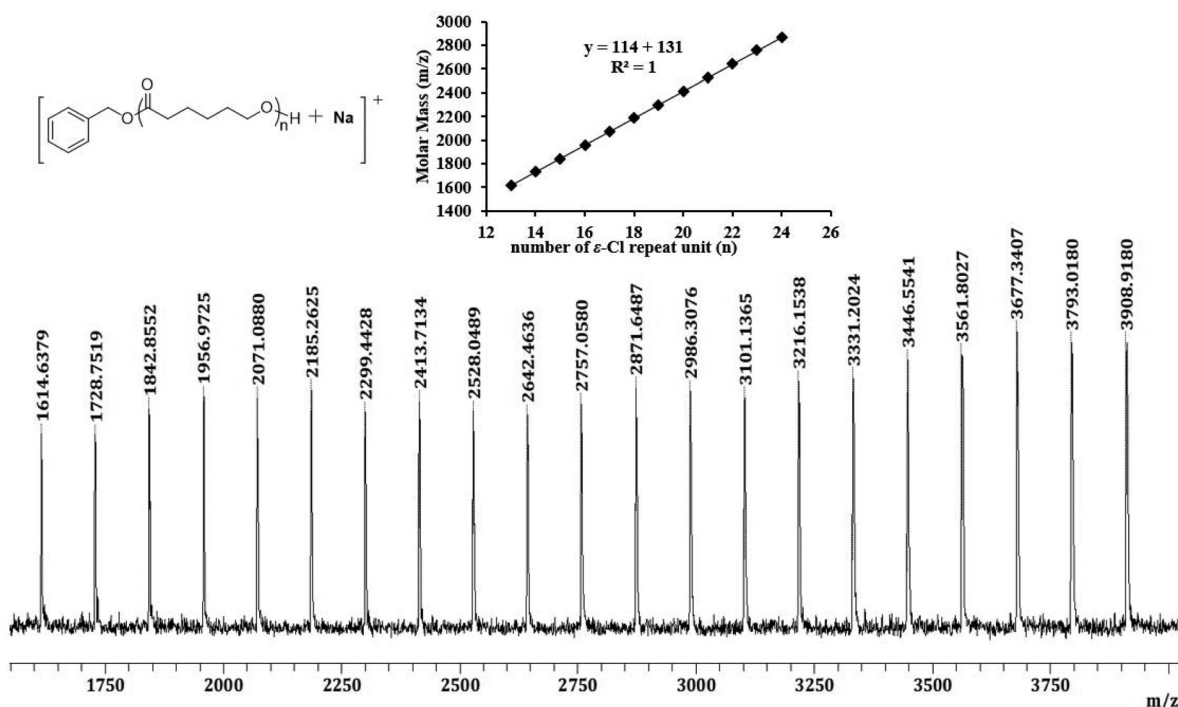


Fig. 8 The MALDI-TOF MS analysis of the resulting PCL produced by Al4/BnOH in toluene at RT.

occurrence of transesterification. In sharp contrast, the MS spectrum of PCL produced by the Al4/BnOH system clearly showed only a series of molecular mass ions (Fig. 8). The linear plot of  $m/z$  values vs. the  $\epsilon$ -CL repeat units ( $n$ ) gave a slope of 114 and an intercept of 131 (inset), which corresponds to a polymer chain structure with BnOH chain-ends. Even 5 h after the full monomer consumption, the mass spectrum of PCL produced by Al4/BnOH still showed one series of peaks with the same slope and intercept without observance of intramolecular cyclization products, which was exactly in line with the fact that Al4/BnOH exhibited the best control over transesterification among the investigated catalyst systems.

## Conclusions

In summary, a series of dimethylaluminum complexes have been synthesized for living ROP of lactones in the presence of the BnOH initiator, producing polyesters with  $M_w$  up to 303 kg mol<sup>-1</sup> and narrow molecular weight distributions ( $D$  value as low as 1.12). The livingness of the ROP has been confirmed with multiple protocols, including predictable polymer  $M_n$  and low  $D$  values, a linear increase of polymer  $M_n$  vs. monomer conversion, a linear increase of polymer  $M_n$  vs. monomer-to-initiator ratio, chain extension experiments, and synthesis of well-defined random, diblock, and triblock copolymers. The combined mechanistic studies including polymerization details, polymerization kinetics, systematic investigation towards the *in situ* NMR reactions and characterization of chain-ends have led to the coordination–insertion mechanism.

The sidearm of ligands demonstrated their significantly important effects on the reactivity of the catalyst. The Al2 catalyst with a butyl substituent on the sidearm exhibited the highest polymerization activity, whereas Al5 with the bulkiest substituent on the sidearm exhibited the lowest one among the investigated catalysts. It is worth noting that the Al4 catalyst system with a rigid pyridine group is robust enough to prevent the occurrence of transesterification and maintain a well-defined block copolymer structure even after heating at 50 °C for 10 h. We anticipate that this strategy should inspire further development of catalyst systems with sidearms for the synthesis of advanced polymers, thus expanding the utility and application of ROP of lactones.

## Conflicts of interest

The authors declare no competing financial interest.

## Acknowledgements

This work was supported by the National Natural Science Foundation of China (Grant No. 21422401, 21374040, 21774042, and 21871107), and the startup funds from Jilin University, Talents Fund of Jilin Province.

## Notes and references

- 1 X. Zhang, M. Fevre, G. O. Jones and R. M. Waymouth, *Chem. Rev.*, 2018, **118**, 839–885.

- 2 M. A. Hillmyer and W. B. Tolman, *Acc. Chem. Res.*, 2014, **47**, 2390–2936.
- 3 O. Dechy-Cabaret, B. Martin-Vaca and D. Bourissou, *Chem. Rev.*, 2004, **104**, 6147–6176.
- 4 M. Labet and W. Thielemans, *Chem. Soc. Rev.*, 2009, **38**, 3484–3504.
- 5 W. N. Ottou, H. Sardon, D. Mecerreyes, J. Vignolle and D. Taton, *Prog. Polym. Sci.*, 2016, **56**, 64–115.
- 6 Y. Li, J. Rodrigues and H. Tomás, *Chem. Soc. Rev.*, 2012, **41**, 2193–2221.
- 7 J.-F. Carpentier, *Organometallics*, 2015, **34**, 4175–4189.
- 8 A. Sauer, A. Kapelski, C. Fliedel, S. Dagonne, M. Kol and J. Okuda, *Dalton Trans.*, 2013, **42**, 9007–9023.
- 9 N. E. Kamber, W. Jeong and R. M. Waymouth, *Chem. Rev.*, 2007, **107**, 5813–5840.
- 10 M. K. Kiesewetter, E. J. Shin, J. L. Hedrick and R. M. Waymouth, *Macromolecules*, 2010, **43**, 2093–2107.
- 11 O. Coulembier, P. Degée, J. L. Hedrick and P. Dubois, *Prog. Polym. Sci.*, 2006, **31**, 723–747.
- 12 C. Thomas and B. Bibal, *Green Chem.*, 2014, **16**, 1687–1699.
- 13 A. P. Dove, *ACS Macro Lett.*, 2012, **1**, 1409–1412.
- 14 C. M. Thomas, *Chem. Soc. Rev.*, 2010, **39**, 165–173.
- 15 J. U. Pothupitiya, N. U. Dharmaratne, T. M. M. Jouaneh, K. V. Fastnacht, D. N. Coderre and M. K. Kiesewetter, *Macromolecules*, 2017, **50**, 8948–8954.
- 16 M. Hong and E. Y.-X. Chen, *Angew. Chem., Int. Ed.*, 2016, **55**, 4188–4193.
- 17 X. Zhang, G. O. Jones, J. L. Hedrick and R. M. Waymouth, *Nat. Chem.*, 2016, **8**, 1047–1053.
- 18 Y. Wei, S. Wang and S. Zhou, *Dalton Trans.*, 2016, **45**, 4471–4485.
- 19 K. M. Osten and P. Mehrkhodavandi, *Acc. Chem. Res.*, 2017, **50**, 2861–2869.
- 20 E. Stirling, Y. Champouret and M. Visseaux, *Polym. Chem.*, 2018, **9**, 2517–2531.
- 21 G. Ceccorulli, M. Scandola, B. K. Ajay Kumar and R. A. Gross, *Biomacromolecules*, 2005, **6**, 902–907.
- 22 A. Kumar, K. Garg and R. A. Gross, *Macromolecules*, 2001, **34**, 3527–3533.
- 23 M. Bouyahyi and R. Duchateau, *Macromolecules*, 2014, **47**, 517–524.
- 24 L. Jasinska-Walc, M. R. Hansen, D. Dudenko, A. Rozanski, M. Bouyahyi, M. Wagner, R. Graf and R. Duchateau, *Polym. Chem.*, 2014, **5**, 3306–3310.
- 25 M. Bouyahyi, M. P. F. Pepels, A. Heise and R. Duchateau, *Macromolecules*, 2012, **45**, 3356–3366.
- 26 L. Jasinska-Walc, M. Bouyahyi, A. Rozanski, R. Graf, M. R. Hansen and R. Duchateau, *Macromolecules*, 2015, **48**, 502–510.
- 27 E. J. Shin, H. A. Brown, S. Gonzalez, W. Jeong, J. L. Hedrick and R. M. Waymouth, *Angew. Chem., Int. Ed.*, 2011, **50**, 6388–6391.
- 28 A. Pilone, N. De Maio, K. Press, V. Venditto, D. Pappalardo, M. Mazzeo, C. Pellicchia, M. Kol and M. Lamberti, *Dalton Trans.*, 2015, **44**, 2157–2165.
- 29 Q. Wang, W. Zhao, J. He, Y. Zhang and E. Y. X. Chen, *Macromolecules*, 2017, **50**, 123–136.
- 30 A. Arbaoui and C. Redshaw, *Polym. Chem.*, 2010, **1**, 801–826.
- 31 C. Redshaw and Y. Tang, *Chem. Soc. Rev.*, 2012, **41**, 4484–4510.
- 32 C. Wang, X.-L. S. Zhi Ma, Y. Gao, Y.-H. Guo, Y. Tang and L.-P. Shi, *Organometallics*, 2006, **25**, 3259–3266.
- 33 C. J. Stephenson, J. P. McInnis, C. Chen, M. P. Weberski, A. Motta, M. Delferro and T. J. Marks, *ACS Catal.*, 2014, **4**, 999–1003.
- 34 T. Liang and C. Chen, *Organometallics*, 2017, **36**, 2338–2344.
- 35 D. J. Jones, V. C. Gibson, S. M. Green and P. J. Maddox, *Chem. Commun.*, 2002, **10**, 1038–1039.
- 36 S. Wang, H.-W. Li and Z. Xie, *Organometallics*, 2004, **23**, 2469–2478.
- 37 S. Wang, H.-W. Li and Z. Xie, *Organometallics*, 2004, **23**, 3780–3787.
- 38 G. Feng, C. Du, L. Xiang, I. del Rosal, G. Li, X. Leng, E. Y. X. Chen, L. Maron and Y. Chen, *ACS Catal.*, 2018, **8**, 4710–4718.
- 39 S. Liao, X. L. Sun and Y. Tang, *Acc. Chem. Res.*, 2014, **47**, 2260–2272.
- 40 X.-Y. Wang, X.-L. Sun, F. Wang and Y. Tang, *ACS Catal.*, 2017, **7**, 4692–4696.
- 41 C. Kan, J. Hu, Y. Huang, H. Wang and H. Ma, *Macromolecules*, 2017, **50**, 7911–7919.
- 42 D. Homden, C. Redshaw, J. A. Wright, D. L. Hughes and M. R. J. Elsegood, *Inorg. Chem.*, 2008, **47**, 5799–5814.
- 43 J. Ma, K. Q. Zhao, M. J. Walton, J. A. Wright, J. W. Frese, M. R. Elsegood, Q. Xing, W. H. Sun and C. Redshaw, *Dalton Trans.*, 2014, **43**, 8300–8310.
- 44 J. Ma, K. Q. Zhao, M. Walton, J. A. Wright, D. L. Hughes, M. R. Elsegood, K. Michiue, X. Sun and C. Redshaw, *Dalton Trans.*, 2014, **43**, 16698–16706.
- 45 I. E. Soshnikov, N. V. Semikolenova, J. Ma, K.-Q. Zhao, V. A. Zakharov, K. P. Bryliakov, C. Redshaw and E. P. Talsi, *Organometallics*, 2014, **33**, 1431–1439.
- 46 P. A. Cameron, V. C. Gibson, C. Redshaw, J. A. Segal, M. D. Bruce, A. J. P. White and D. J. Williams, *Chem. Commun.*, 1999, 1883–1884.
- 47 M. Li, M. Chen and C. Chen, *Polymer*, 2015, **64**, 234–239.
- 48 D. Zhang, W. Pang and C. Chen, *J. Organomet. Chem.*, 2017, **836**, 56–61.
- 49 W.-L. Kong, Z.-Y. Chai and Z.-X. Wang, *Dalton Trans.*, 2014, **43**, 14470–14480.
- 50 J. B. L. Gallaway, J. R. K. McRae, A. Decken and M. P. Shaver, *Can. J. Chem.*, 2012, **90**, 419–426.
- 51 C.-T. Chen, C.-A. Huang and B.-H. Huang, *Dalton Trans.*, 2003, **1**, 3799–3803.
- 52 C.-T. Chen, C.-A. Huang and B.-H. Huang, *Macromolecules*, 2004, **37**, 7968–7973.

- 53 N. Iwasa, J. Liu and K. Nomura, *Catal. Commun.*, 2008, **9**, 1148–1152.
- 54 N. Iwasa, S. Katao, J. Liu, M. Fujiki, Y. Furukawa and K. Nomura, *Organometallics*, 2009, **28**, 2179–2187.
- 55 W. Yang, K. Q. Zhao, T. J. Prior, D. L. Hughes, A. Arbaoui, M. R. Elsegood and C. Redshaw, *Dalton Trans.*, 2016, **45**, 11990–12005.
- 56 X. Wang, K.-Q. Zhao, Y. Al-Khafaji, S. Mo, T. J. Prior, M. R. J. Elsegood and C. Redshaw, *Eur. J. Inorg. Chem.*, 2017, **13**, 1951–1965.
- 57 S. K. Roymuhury, D. Chakraborty and V. Ramkumar, *Eur. Polym. J.*, 2015, **70**, 203–214.
- 58 C. K. Williams, L. E. Breyfogle, S. K. Choi, W. Nam, V. G. Young Jr., M. A. Hillmyer and W. B. Tolman, *J. Am. Chem. Soc.*, 2003, **125**, 11350–11359.
- 59 P. A. Cameron, V. C. Gibson, C. Redshaw, J. A. Segal, A. J. P. White and D. J. Williams, *Dalton Trans.*, 2002, **1**, 415–422.
- 60 W. Li, W. Wu, Y. Wang, Y. Yao, Y. Zhang and Q. Shen, *Dalton Trans.*, 2011, **40**, 11378–11381.
- 61 C. Bakewell, T. P. Cao, N. Long, X. F. Le Goff, A. Auffrant and C. K. Williams, *J. Am. Chem. Soc.*, 2012, **134**, 20577–20580.
- 62 W.-H. Sun, M. Shen, W. Zhang, W. Huang, S. Liua and C. Redshaw, *Dalton Trans.*, 2011, **40**, 2645–2653.
- 63 W.-A. Ma and Z.-X. Wang, *Dalton Trans.*, 2011, **40**, 1778–1786.
- 64 H. C. Tseng, M. Y. Chiang, W. Y. Lu, Y. J. Chen, C. J. Lian, Y. H. Chen, H. Y. Tsai, Y. C. Lai and H. Y. Chen, *Dalton Trans.*, 2015, **44**, 11763–11773.
- 65 D. Li, Y. Peng, C. Geng, K. Liu and D. Kong, *Dalton Trans.*, 2013, **42**, 11295–11303.
- 66 N. Nomura, A. Taira, A. Nakase, T. Tomioka and M. Okada, *Tetrahedron*, 2007, **63**, 8478–8484.
- 67 Y.-B. Jia, Y.-B. Wang, W.-M. Ren, T. Xu, J. Wang and X.-B. Lu, *Macromolecules*, 2014, **47**, 1966–1972.
- 68 J. He, Y. Zhang, L. Falivene, L. Caporaso, L. Cavallo and E. Y. X. Chen, *Macromolecules*, 2014, **47**, 7765–7774.
- 69 Q. Wang, W. Zhao, S. Zhang, J. He, Y. Zhang and E. Y. X. Chen, *ACS Catal.*, 2018, **8**, 3571–3578.